The Reaction Mass Biped: Equations of Motion, Hybrid Model for Walking and Trajectory Tracking Control

Koushil Sreenath and Amit K. Sanyal

***Abstract*— Pendulum models have been studied as benchmark problems for development of nonlinear control schemes, as well as reduced-order models for the dynamics analysis of locomotion of humanoid robots. This work provides a generalization of the previously introduced *Reaction Mass Pendulum (RMP)*, which is a multibody inverted pendulum model, to a bipedal model that can better model bipedal locomotion. The RMP consists of an extensible "leg" and a "body" with moving proof masses that give rise to a variable rotational inertia. The Reaction Mass Biped (RMB) introduced here has two legs, one of which takes the role of a stance leg and the other performs as a swing leg during bipedal locomotion. The bipedal walking dynamics model of the RMB is therefore hybrid, with the roles of stance leg and swing leg interchanged after each cycle. The dynamics model is developed using a variational mechanics approach, without using generalized coordinates for the rotational degrees of freedom. This dynamics model has thirteen degrees of freedom, all of which are considered to be actuated in the control design. A set of desired state trajectories that can enable bipedal walking in straight and curved lines are generated. A control scheme is then designed for asymptotically stable tracking of this set of trajectories with an almost global domain of attraction. Numerical simulation results confirm the stability of this tracking control scheme for different walking trajectories of the RMB.**

I. Introduction

In order to model bipedal locomotion for general planar trajectories covered by a moving biped, an extension of the Reaction Mass Pendulum (RMP) model developed in [1], [2], [3] is considered here. This extension adds a swing leg to the RMP model in [1], [2], [3], and this model is termed the Reaction Mass Biped (RMB). The dynamics of this biped model is necessarily a hybrid dynamics model for bipedal motion. This document details the continuous-time stance dynamics with one foot on the ground, the continuous-time extended dynamics with both feet off the ground, the discrete-time impact model when the swing foot hits the ground, and finally the hybrid model of walking for the reaction mass biped. In all these cases, we derive the dynamics directly through application of the Lagrange-d'Alembert principle, by considering variations on the configuration manifolds for these dynamics. This leads to formulation of the dynamics without using local (generalized) coordinates for the rotational degrees of freedom. One advantage of this formulation is that it can effectively handle rotations of the ankle and hip joints as well as the torso of the RMB without encountering kinematic singularities. Another advantage is the control scheme formulated based on this dynamics model is asymptotically stable with a large domain of attraction.

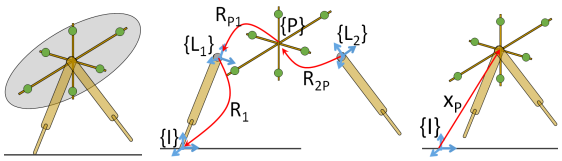

(a) RMB (b) Rotations (c) Extended

Fig. 1: Reaction Mass Biped (RMB)

Reduced-order models of bipedal gait of humanoid robots include various versions of the inverted pendulum model, such as the 2D and 3D linear inverted pendulums (LIP)[4], [5], the cart-table model [6], the variable impedance LIP [7], the spring-loaded inverted pendulum[8], and the angular momentum pendulum model (AMPM) [9], [10]. A limitation of the above models is that they do not characterize the time-varying rotational inertia. Consequences of neglecting the rotational inertia is that the angular momentum of the system about its CoM must be zero and the ground reaction force (GRF) must be directed along the lean line. Humanoid robots have no reason to obey these artificial conditions, and it has been reported that even during human gait at normal speed, the GRF diverges from the lean line[2] and this may be important for maintaining balance. A variable inertia is also essential for balance control, and highly dynamic motions like jumping and diving [3]. The Reaction Mass Pendulum (RMP) model was introduced in [1] as a three-dimensional inverted pendulum model with variable inertia, which could be used as a reduced-order model for humanoid motion that accounted for the variable inertia and angular momentum of a humanoid body. This model consists of a variable length "leg" and a variable inertia "body".

The Reaction Mass Biped introduced in this paper further develops this notion by adding bipedal hybrid dynamics that is crucial to stable and robust bipedal locomotion. There is significant work in the formal stabilization of 3D walking using techniques based on controlled symmetries and Routhian reduction [11], [12], [13], and on hybrid zero dynamics [14], [15]. These methods have been extended to yaw steering of 3D robots [16]. Figure 1 illustrates the Reaction Mass Biped in stance. The variables used to describe the dynamics of the RMB are summarized in Table I.

K. Sreenath is with the faculty of Mechanical Engineering, Carnegie Mellon University, Pittsburgh, PA 15213, USA koushils@cmu.edu

A. K. Sanyal is with the faculty of Mechanical and Aerospace Engineering, New Mexico State University, Las Cruces, NM 88003, USA asanyal@nmsu.edu

$m_L \in \mathbb{R}$	Mass of either Leg at Hip Joint
$m_P \in \mathbb{R}$	Mass of Reaction masses
$m \in \mathbb{R}$	Mass of the entire system
$J_{L_0} \in \mathbb{R}^{3\times3}$	Inertia matrix of either leg w.r.t the body frame when leg length is its nominal value ρ_0
$J_{P_0} \in \mathbb{R}^{3\times3}$	Inertia matrix of the torso w.r.t the body frame
$\{I\}$	Inertial frame at the stance foot
$\{L_1\}$	Body frame of the stance leg at the hip joint
$\{P\}$	Body frame of the torso at the hip joint
$\{L_2\}$	Body frame of the swing leg at the hip joint
$\rho_1 \in C$	Distance between CoM of the stance leg and its ankle
$\rho_0 \in C$	Distance between CoM of the swing leg and its ankle
$R_P \in SO(3)$	Rotation matrix of the torso from the body frame to the inertial frame {I}
$R_{P1} \in SO(3)$	Rotation matrix of the torso from the body frame {P} to the stance leg body frame {L1}
$R_{2P} \in SO(3)$	Rotation matrix of the swing leg from the body frame {L2} to the torso body frame {P}
$\Omega_1 \in \mathbb{R}^3$	Angular velocity of the stance leg in the body frame
$\Omega_2 \in \mathbb{R}^3$	Angular velocity of the swing leg in the body frame
$\Omega_P \in \mathbb{R}^3$	Angular velocity of the torso in the body frame
$s_i \in S$	Position of the i'th reaction mass
$e_3 \in \mathbb{R}^3$	Standard unit vector along the gravity direction (downward) in the inertial frame

TABLE I: Enumeration of the symbols used in the paper.

II. Mathematical Model

A. Stance Dynamics

A coordinate-free dynamics model is developed for the stance phase of the Reaction Mass Biped, using rotation matrices to represent the attitudes of the two legs, R_1, R_2, and the torso, R_P, along with scalars ρ_1, ρ_2 to represent the length of the two legs, and s_i to represent the position of the i^th pair of reaction masses. During the stance phase, the stance leg is assumed to be pinned to the ground. The configuration manifold of the system is given by $\mathcal{Q}_s = C \times SO(3) \times SO(3) \times SO(3) \times S \times C$, with $\rho_1, \rho_2 \in C = [0, r]$, $R_1, R_P, R_2 \in SO(3)$, $s = \begin{bmatrix} s_1 & s_2 & s_3 \end{bmatrix}^{\mathrm{T}} \in S$. The symbols used in this paper are tabulated in Table I.

We have the following rotational kinematic relations: $\dot{R}_1 = R_1\hat{\Omega}_1$, $\dot{R}_{P1} = R_{P1}\hat{\Omega}_{P1}$, $\dot{R}_P = R_P\hat{\Omega}_P$, $\dot{R}_{2P} = R_{2P}\hat{\Omega}_{2P}$, $\dot{R}_2 = R_2\hat{\Omega}_2$, where $\Omega_1, \Omega_2, \Omega_P$ are the respective body angular velocities, and are related by

$$\Omega_P = \Omega_{P1} + R_{P1}^{\mathrm{T}}\Omega_1, \quad \text{where} \quad R_{P1} = R_1^{\mathrm{T}}R_P, \tag{1}$$

$$\Omega_2 = \Omega_{2P} + R_{2P}^{\mathrm{T}}\Omega_P, \quad \text{where} \quad R_{2P} = R_P^{\mathrm{T}}R_2. \tag{2}$$

The expression for the kinetic energy of the system, $\mathcal{T}_s : T\mathcal{Q}_s \to \mathbb{R}$, is given by

$$\begin{aligned}\mathcal{T}_s &= \frac{1}{2}m\dot{\rho}_1^2 + \sum_{i=1}^{3} m_p\dot{s}_i^2 + \frac{1}{2}\Omega_1^T J_1(\rho_1)\Omega_1 + \\ &\quad \frac{1}{2}\Omega_P^T J_P(s)\Omega_P + \frac{1}{2}\Omega_2^T J_{L_0}\Omega_2, \text{ where}\end{aligned} \tag{3}$$

$$J_1(\rho_1) = J_{L_0} + K_1(\rho_1), \qquad K_1(\rho_1) = -m\rho_1^2(e_3^\times)^2$$

$$J_P(s) = J_{P_0} + K_P(s), \qquad K_P(s) = -2\sum_{i=1}^{3} m_p s_i^2(e_i^\times)^2.$$

The potential energy $\mathcal{U}_s : \mathcal{Q}_s \to \mathbb{R}$ due to uniform gravity is

$$\mathcal{U}_s = -mg\rho_1 R_1^T e_3 \cdot e_3. \tag{4}$$

Note that the negative sign arises due to our convention of e_3 being along the gravitational direction. The Lagrangian of the system $\mathcal{L}_s : T\mathcal{Q}_s \to \mathbb{R}$ is then given by $\mathcal{L}_s = \mathcal{T}_s - \mathcal{U}_s$. The equations of motion can then be obtained by applying the Lagrange-d'Alembert principle:

$$\begin{aligned}\int \Big(&\delta\mathcal{L}_s + \eta_1^{\mathrm{T}}\tau_1 + f_1\delta\rho_1 + \eta_{P1}^{\mathrm{T}}\tau_{D_1} \\ &+ \sum_{i=1}^{3} u_i\delta s_i + \eta_{P2}^{\mathrm{T}}\tau_{D_2}\Big) = 0,\end{aligned} \tag{5}$$

where the first term in the integral represents the variation of the Lagrangian, computed using reduced variations on SO(3) [17]. Define

$$\begin{aligned}N(s,\dot{s}) &= \frac{\mathrm{d}}{\mathrm{d}t}K_P(s) = 4m_p \,\mathrm{diag}\,\{s_2\dot{s}_2 + s_3\dot{s}_3, \\ &\quad s_1\dot{s}_1 + s_3\dot{s}_3, s_1\dot{s}_1 + s_2\dot{s}_2\}, \quad \text{and } L(s,\Omega_P) \\ &= \frac{\partial}{\partial s}(\frac{1}{2}\,\Omega_P^{\mathrm{T}}\,K_P(s)\,\Omega_P) = 2m_p\begin{bmatrix} s_1(\Omega_{P_2}^2 + \Omega_{P_3}^2) \\ s_2(\Omega_{P_3}^2 + \Omega_{P_1}^2) \\ s_3(\Omega_{P_1}^2 + \Omega_{P_2}^2)\end{bmatrix}\end{aligned} \tag{6}$$

Then the dynamics equations of motion can be compactly expressed (useful for the impact model) by defining $\boldsymbol{q}_s = (\rho_1, R_1, R_P, s, R_2)$, and $\boldsymbol{\omega}_s = \begin{bmatrix}\dot{\rho}_1 & \Omega_1 & \Omega_P & \dot{s} & \Omega_2\end{bmatrix}^T$:

$$\boldsymbol{D}_s(\boldsymbol{q}_s)\boldsymbol{\omega}_s + \boldsymbol{H}_s(\boldsymbol{q}_s, \boldsymbol{\omega}_s) = \boldsymbol{B}_s\boldsymbol{u}_s, \tag{7}$$

where, $\boldsymbol{D}_s(\boldsymbol{q}_s) = \mathrm{diag}\,(m, J_1(\rho_1), J_P(s), 2m_pI, J_{L_0})$, and

$$\boldsymbol{H}_s(\boldsymbol{q}_s, \boldsymbol{\omega}_s) = \begin{bmatrix} -m\rho_1\Omega_1^T(e_3^\times)^2\Omega_1 \\ -\Omega_1 \times J_1(\rho_1)\Omega_1 + 2m\rho_1\dot{\rho}_1(e_3^\times)^2\Omega_1 + mg\rho_1 e_3^\times R_1^T e_3 \\ -\Omega_P \times J_P(s)\Omega_P + 4\sum_{i=1}^{3} m_p s_i\dot{s}_i(e_i^\times)^2\Omega_P \\ -L(s,\Omega_P) \\ -\Omega_2 \times J_{L_0}\Omega_2 \end{bmatrix},$$

$$\boldsymbol{B}_s(\boldsymbol{q}_s) = \begin{bmatrix} I & 0 & 0 & 0 & 0 \\ 0 & I & -R_1^T R_P & 0 & 0 \\ 0 & 0 & I & 0 & -R_P^T R_2 \\ 0 & 0 & 0 & I & 0 \\ 0 & 0 & 0 & 0 & I \end{bmatrix}, \boldsymbol{u}_s = \begin{bmatrix} f_1 \\ \tau_1 \\ \tau_{D1} \\ u_s \\ \tau_{D2} \end{bmatrix}.$$

***Remark* 1.** *Note that the stance dynamics of the Reaction Mass Biped is fully actuated.*

B. Extended Dynamics

In the extended dynamics model, the foot is no longer pinned to the ground unlike the stance dynamics. The extended model is illustrated in Figure 1c, and has the configuration manifold $\mathcal{Q}_e = \mathbb{R}^3 \times SO(3) \times SO(3) \times S \times SO(3)$. The kinetic and potential energies, $\mathcal{T}_e : T\mathcal{Q}_e \to \mathbb{R}, \mathcal{U}_e : Q_e \to \mathbb{R}$ can be derived as in the stance dynamics, resulting in:

$$\begin{aligned}\mathcal{T}_e &= \frac{1}{2}m\dot{x}_P \cdot \dot{x}_P + \sum_{i=1}^{3} m_p\dot{s}_i^2 + \frac{1}{2}\Omega_1^T J_{L_0}\Omega_1 \\ &\quad + \frac{1}{2}\Omega_P^T J_P(s)\Omega_P + \frac{1}{2}\Omega_2^T J_{L_0}\Omega_2,\end{aligned} \tag{8}$$

$$\mathcal{U}_e = -mgx_P \cdot e_3. \tag{9}$$

The equations of motion can be obtained through application of the Lagrange-d'Alembert principle as outlined earlier. We will directly write this in matrix form by first defining, $\boldsymbol{q}_e = \begin{bmatrix} R_1 & R_P & s & R_2 & x_P \end{bmatrix}^T$, and $\boldsymbol{\omega}_e = \begin{bmatrix} \Omega_1 & \Omega_P & \dot{s} & \Omega_2 & \dot{x}_P \end{bmatrix}^T$, where x_P is the position of the hip in the inertial frame. We then have,

$$\boldsymbol{D}_e(\boldsymbol{q}_e)\boldsymbol{\omega}_e + \boldsymbol{H}_e(\boldsymbol{q}_e, \boldsymbol{\omega}_e) = \boldsymbol{B}_e(\boldsymbol{q}_e)\boldsymbol{u}_e,$$

where, $\boldsymbol{D}_e(\boldsymbol{q}_e) = diag\left(J_{L_0}, J_P(s), 2m_pI, J_{L_0}, m\right)$,

$$\boldsymbol{H}_e(\boldsymbol{q}_e, \boldsymbol{\omega}_e) = \begin{bmatrix} -\Omega_1 \times J_{L_0}\Omega_1 \\ -\Omega_P \times J_P(s)\Omega_P + 4\sum_{i=1}^{3} m_p s_i \dot{s}_i (e_i^{\times})^2 \Omega_P \\ -L(s, \Omega_P) \\ -\Omega_2 \times J_{L_0}\Omega_2 \\ mge_3 \end{bmatrix}, \quad (10)$$

$$\boldsymbol{B}_e(\boldsymbol{q}_e) = \begin{bmatrix} -R_1^T R_P & 0 & 0 \\ I & 0 & -R_1^T R_P \\ 0 & I & 0 \\ 0 & 0 & 0 \end{bmatrix}, \quad \boldsymbol{u}_e = \begin{bmatrix} \tau_{D1} \\ u_s \\ \tau_{D2} \end{bmatrix}. \quad (11)$$

***Remark* 2.** *Note that the extended dynamics model of the reaction mass biped is underactuated. This is in contrast to the stance dynamics model, which is fully actuated.*

C. Impact Model

The discrete-time impact model captures the impact of the swing foot with the ground, resulting in instantaneous changes in joint velocities. To capture this, map the stance coordinates to the extended coordinates, perform the impact in extended coordinates, and then map the extended coordinates to stance coordinates while relabeling the old swing leg as the new stance leg. To map stance coordinates to extended coordinates, express $x_P, \dot{x}_P$ in terms of stance coordinates. As the stance foot is on the ground, $x_P = \rho_1 R_1 e_3$ and $\dot{x}_P = -\dot{\rho}_1 R_1 e_3 - \rho_1 R_1 \Omega_1^{\times} e_3$. This is expressed by the map:

$$\boldsymbol{q}_e = \Upsilon^{\boldsymbol{q}}_{s\to e}(\boldsymbol{q}_s), \quad \boldsymbol{\omega}_e = \Upsilon^{\boldsymbol{\omega}}_{s\to e}(\boldsymbol{\omega}_s).$$

Denote the map from extended to stance coordinates by:

$$\boldsymbol{q}_s = \Upsilon^{\boldsymbol{q}}_{e\to s}(\boldsymbol{q}_e), \quad \boldsymbol{\omega}_s = \Upsilon^{\boldsymbol{\omega}}_{e\to s}(\boldsymbol{\omega}_e).$$

This map computes ρ_1 from x_P as, $\rho_1 = ||x_P||$.

To model the impact map, consider $(\boldsymbol{q}_e^-, \boldsymbol{\omega}_e^-)$ as the state before impact, $(\boldsymbol{q}_e^+, \boldsymbol{\omega}_e^+)$ the state after impact, and F_{ext} as the external force. Then use the following relation from [18]:

$$\boldsymbol{D}(\boldsymbol{q}_e^+)\boldsymbol{\omega}_e^+ - \boldsymbol{D}(\boldsymbol{q}_e^-)\boldsymbol{\omega}_e^- = F_{ext}.$$

Further, the swing foot position and velocity are given as,

$$x_{F_2} = x_P + \rho_2^{td} R_2 e_3, \qquad \dot{x}_{F_2} = \dot{x}_P - \rho_2^{td} R_2 (e_3)^{\times} \Omega_2,$$

where ρ_2^{td} is the instantaneous value of ρ_2 at touchdown. The post impact swing foot velocity is $\dot{x}_{F_2}^+ = 0$, as this foot becomes the new stance foot. This is expressed as

$$A\boldsymbol{\omega}_e^+ = 0 \text{ where } A = \begin{bmatrix} 0 & -\rho_2^{td} R_2^+ (e_3)^{\times} & 0 & 0 & I \end{bmatrix}.$$

Further, denoting I_R as the impact force at the swing foot, we have $F_{ext} = A^T I_R$. The above equations are expressed in matrix form to solve for $\boldsymbol{\omega}_e^+$ and I_R,

$$\begin{bmatrix} \boldsymbol{\omega}_e^+ \\ I_R \end{bmatrix} = \begin{bmatrix} \boldsymbol{D}_e(\boldsymbol{q}_e^+) & -A^T \\ A & 0 \end{bmatrix}^{-1} \begin{bmatrix} -\boldsymbol{D}_e(\boldsymbol{q}_e^-)\boldsymbol{\omega}_e^- \\ 0 \end{bmatrix}. \quad (12)$$

This defines a map Γ such that $\boldsymbol{\omega}_e^+ = \Gamma(\boldsymbol{\omega}_e^-)$.

The impact map is then defined by the map $\Delta_{s\to s} : \mathcal{S} \to TQ$, where $\mathcal{S} = \{x_s \in TQ_s \mid (\rho_2 R_2 e_3 - \rho_1 R_1 e_3) \cdot e_3 = 0\}$ is the switching surface representing the contact of the swing leg foot with the ground. We express

$$\Delta_{s\to s} := \begin{bmatrix} \Delta^{\boldsymbol{q}}_{s\to s} \\ \Delta^{\boldsymbol{\omega}}_{s\to s} \end{bmatrix},$$

where the components $\Delta^{\boldsymbol{q}}_{s\to s}$ and $\Delta^{\boldsymbol{\omega}}_{s\to s}$ define the transition maps for the configuration variables and their velocities, respectively. These transition maps are obtained from the above equations as follows:

$$\begin{aligned} \Delta^{\boldsymbol{q}}_{s\to s} &:= \Upsilon^{\boldsymbol{q}}_{e\to s} \circ \mathcal{R} \circ \Upsilon^{\boldsymbol{q}}_{s\to e}, \\ \Delta^{\boldsymbol{\omega}}_{s\to s} &:= \Upsilon^{\boldsymbol{\omega}}_{e\to s} \circ \mathcal{R} \circ \Gamma \circ \Upsilon^{\boldsymbol{\omega}}_{s\to e}, \end{aligned}$$

where $\mathcal{R}$ represents coordinate relabeling such that the old swing leg is labeled as the new stance leg and vice-versa.

D. Hybrid Model for Walking

The hybrid model for walking is based on the stance dynamics and the impact model developed in the previous sections, and can be represented as follows:

$$\Sigma : \begin{cases} \dot{\boldsymbol{D}_s}\boldsymbol{\omega}_s = \boldsymbol{H}_s(\boldsymbol{q}_s, \boldsymbol{\omega}_s) + \boldsymbol{B}_s(\boldsymbol{q}_s)\boldsymbol{u}_s, & (\boldsymbol{q}_s^-, \boldsymbol{\omega}_s^-) \notin \mathcal{S}, \\ (\boldsymbol{q}_s^+, \boldsymbol{\omega}_s^+) = \Delta_{s\to s}(\boldsymbol{q}_s^-, \boldsymbol{\omega}_s^-), & (\boldsymbol{q}_s^-, \boldsymbol{\omega}_s^-) \in \mathcal{S}. \end{cases}$$

III. Actuation and Controlled Motion

A. Motion Planning for Moving between Ground Locations

Consider a trajectory connecting two ground points with given initial and final velocities, such that it avoids fixed obstacles. The projection of the motion of the center of mass of the torso on the horizontal (ground) plane should closely follow this trajectory. Assuming that this trajectory is known a priori, a stride length that is optimal (or natural) for the RMB is used to determine the number of steps required to cover the generated trajectory. If l_s is the optimal stride length and p_l is the path length of the trajectory, then the nearest integer to p_l/l_s is used as the number of strides required to cover this trajectory. Motion primitives for the RMB legs in time interval $[0, T]$ are given by:

$$\begin{aligned} &\rho_1^d = \rho_0 + \bar{\rho}\sin(\omega t),\ \omega = \frac{\pi}{T},\ \rho_0 > \bar{\rho} > 0, \\ &R_1^d = R_{1_0} \exp\left(\zeta_1^{\times} \sin(\omega t/2)\right), \\ &\rho_2^d = \rho_0, \\ &R_2^d = R_{2_0} \exp\left(\zeta_2^{\times} \sin(\omega t/2)\right). \end{aligned} \quad (13)$$

Note that the constant vectors $\zeta_1, \zeta_2 \in \mathbb{R}^3$ for the leg rotation axes could be equal. Similarly, $R_{1_0}, R_{2_0} \in \mathrm{SO}(3)$ are equal when the biped is standing erect, and ρ_0 and $\bar{\rho}$ are set

according to the calculated stride length. Motion primitives for the torso over the time interval $[0, T]$ are:

$$\begin{aligned} R_P^d &= R_1^d \exp\Big(\gamma \log\big((R_1^d)^{\mathrm{T}} R_2^d\big)\Big),\ \gamma \in [0,1], \\ s^d &= s_0 + \bar{s}\sin(\omega t), \end{aligned} \tag{14}$$

where $s_0, \bar{s} \in \mathbb{R}^3$ give the appropriate inertia distribution for the torso with $|s_{0i}| > |\bar{s}_i|$, $\log : \mathrm{SO}(3) \to \mathfrak{so}(3)$ is the logarithm map that is inverse of the matrix exponential, and γ is a weight factor. Note that $R_P^d = R_1^d$ when $\gamma = 0$ and $R_P^d = R_2^d$ when $\gamma = 1$. These weights can be used to mimic human bipedal gait, where the body (torso) becomes more closely aligned with the stance leg as the speed of bipedal motion increases. By making γ and ω time-varying, one can transition between different speeds of bipedal motion.

The stride length is given by the horizontal distance traversed by the ankle joint of a leg during a single swing phase. The inertial position of the ankle/foot of the swing leg at an instant is given by

$$a_{L2} = a_{L1} + \rho_1 R_1 e_3 - \rho_2 R_2 e_3, \tag{15}$$

where a_{L1}, a_{L2} denote the positions of the ankles of the stance and swing leg, respectively. With the coordinate frames as illustrated in Fig. 1 and substituting equation (13) for the desired motion trajectories, the start and end positions of the swing foot during a cycle are:

$$\begin{aligned} a_{L2}^s &= a_{L1} + \rho_0 R_{1_0} e_3 - \rho_0 R_{2_0} e_3, \\ a_{L2}^e &= a_{L1} + \rho_0 R_{1_0} \exp(\zeta_1^\times) e_3 - \rho_0 R_{2_0} \exp(\zeta_2^\times) e_3 \end{aligned} \tag{16}$$

Therefore the stride displacement is given by

$$a_{L2}^e - a_{L2}^s = \rho_0 R_{1_0}\big(\exp(\zeta_1^\times) - I\big)e_3 + \rho_0 R_{2_0}\big(I - \exp(\zeta_2^\times)\big)e_3. \tag{17}$$

Using Rodrigues' rotation formula, (17) can be simplified to

$$\begin{aligned} v_s^d = \rho_0 R_{1_0}\big\{\hat{\zeta}_1^\times \sin\|\zeta_1\| + \big(\hat{\zeta}_1^\times\big)^2(1 - \cos\|\zeta_1\|)\big\}e_3 \\ - \rho_0 R_{2_0}\big\{\hat{\zeta}_2^\times \sin\|\zeta_2\| + \big(\hat{\zeta}_2^\times\big)^2(1 - \cos\|\zeta_1\|)\big\}e_3, \end{aligned} \tag{18}$$

where v_s^d denotes the stride displacement, and $\hat{\zeta}_1, \hat{\zeta}_2$ denote the unit vectors along ζ_1, ζ_2 respectively. This sets the desired stride length to $l_s^d = \|v_s^d\|$. Note that the constraint $e_3^{\mathrm{T}} v_s^d = 0$ is a constraint on R_{1_0}, R_{2_0}, ζ_1 and ζ_2. Substituting (18) for v_s^d, this constraint is expressed as

$$\begin{aligned} &\Gamma_{1_0}^{\mathrm{T}}\big\{\hat{\zeta}_1^\times \sin\|\zeta_1\| + \big(\hat{\zeta}_1^\times\big)^2(1 - \cos\|\zeta_1\|)\big\}e_3 = \\ &\Gamma_{2_0}^{\mathrm{T}}\big\{\hat{\zeta}_2^\times \sin\|\zeta_2\| + \big(\hat{\zeta}_2^\times\big)^2(1 - \cos\|\zeta_1\|)\big\}e_3, \\ &\text{where } \Gamma_{1_0} = R_{1_0}^{\mathrm{T}} e_3,\ \Gamma_{2_0} = R_{2_0}^{\mathrm{T}} e_3. \end{aligned} \tag{19}$$

Expression (19) is satisfied by setting

$$\zeta_1 = \zeta_2 \text{ and } R_{2_0} = \exp(\theta e_3^\times) R_{1_0}, \tag{20}$$

for $\theta \in \mathbb{S}^1$. The second equality in (20) guarantees that $\Gamma_{1_0} = \Gamma_{2_0}$. Substituting (20) in (13), one obtains:

$$\begin{aligned} (R_1^d)^{\mathrm{T}} R_2^d &= \exp\big(-c(t)\zeta_1^\times\big) R_{1_0}^{\mathrm{T}} R_{2_0} \exp\big(c(t)\zeta_1^\times\big) \\ &= \exp\big(-c(t)\zeta_1^\times\big) \exp\big(\theta (R_{1_0}^{\mathrm{T}} e_3)^\times\big) \exp\big(c(t)\zeta_1^\times\big) \\ &= \exp\Big(\theta\big(\exp(-c(t)\zeta_1^\times) R_{1_0}^{\mathrm{T}} e_3\big)^\times\Big) \end{aligned} \tag{21}$$

where $c(t) = \sin(\omega t/2)$. The above simplification uses the following relation multiple times:

$$R^{\mathrm{T}} \exp(\phi e^\times) R = \exp\big(\phi (R^{\mathrm{T}} e)^\times\big),$$

for $e \in \mathbb{S}^2$. Substituting (21) into (14) gives:

$$R_P^d = R_1^d \exp\Big(\gamma\theta\big(\exp(-c(t)\zeta_1^\times) R_{1_0}^{\mathrm{T}} e_3\big)^\times\Big), \tag{22}$$

which can be expanded using Rodrigues' formula.

B. Trajectory Tracking Control Scheme

Define the trajectory tracking errors:

$$\begin{aligned} &\tilde{\rho}_1 = \rho_1 - \rho_1^d, \quad \dot{\tilde{\rho}}_1 = \frac{\mathrm{d}}{\mathrm{d}t}\tilde{\rho}_1, \\ &Q_1 = R_1 (R_1^d)^{\mathrm{T}}, \quad \tilde{\Omega}_1 = \Omega_1 - \Omega_1^d, \\ &Q_P = R_P (R_P^d)^{\mathrm{T}}, \quad \tilde{\Omega}_P = \Omega_P - \Omega_P^d, \\ &\tilde{s} = s - s^d, \quad \dot{\tilde{s}} = \frac{\mathrm{d}}{\mathrm{d}t}\tilde{s}, \\ &Q_2 = R_2 (R_2^d)^{\mathrm{T}}, \quad \tilde{\Omega}_2 = \Omega_2 - \Omega_2^d. \end{aligned} \tag{23}$$

Generalizing the trajectory tracking control scheme in [3], a Lyapunov function candidate is defined for the stance leg:

$$\begin{aligned} V_{L_1}(\rho_1, \tilde{\rho}_1, Q_1, \dot{\tilde{\rho}}_1, \tilde{\Omega}_1) = \frac{1}{2} m \dot{\tilde{\rho}}_1^2 + \frac{1}{2}\tilde{\Omega}_1^{\mathrm{T}} J_1(\rho_1)\tilde{\Omega}_1 + \frac{1}{2} k \tilde{\rho}_1^2 \\ + \Phi\big(\mathrm{tr}(A - A Q_1)\big), \end{aligned} \tag{24}$$

where $k > 0$, $A = \mathrm{diag}(a_1, a_2, a_3)$ with $a_1 > a_2 > a_3 > 0$. $\Phi : \mathbb{R} \to \mathbb{R}$ is a $\mathcal{C}^2$ function that satisfies $\Phi(0) = 0$, $\Phi'(x) > 0$ for all $x \in \mathbb{R}^+$. and $\Phi'(\cdot) \le \alpha(\cdot)$, where $\alpha(\cdot)$ is Class-$\mathcal{K}$ [19]. The Lyapunov function candidate for the torso is:

$$\begin{aligned} V_P(Q_P, \tilde{\Omega}_P, s, \tilde{s}, \dot{\tilde{s}}) = \frac{1}{2}\tilde{\Omega}_P^{\mathrm{T}} J_P(s)\tilde{\Omega}_P + m_p \dot{\tilde{s}}^{\mathrm{T}}\dot{\tilde{s}} + \frac{1}{2}\tilde{s}^{\mathrm{T}} P \tilde{s} \\ + \Phi\big(\mathrm{tr}(A - A Q_P)\big). \end{aligned} \tag{25}$$

The Lyapunov function candidate for the swing leg is:

$$V_{L_2}(Q_2, \tilde{\Omega}_2) = \frac{1}{2}\tilde{\Omega}_2^{\mathrm{T}} J_{L_0}\tilde{\Omega}_2 + \Phi\big(\mathrm{tr}(A - A Q_2)\big), \tag{26}$$

where J_{L_0} is the inertia of the swing leg at its nominal length (ρ_0), which is kept constant during swing phase. The time derivatives of these Lyapunov functions along the stance dynamics of the RMB system are evaluated.

The time derivative of V_{L_1} along stance dynamics (7) is:

$$\begin{aligned} &\frac{\mathrm{d}}{\mathrm{d}t} V_{L_1}(\rho_1, \tilde{\rho}_1, Q_1, \dot{\tilde{\rho}}_1, \tilde{\Omega}_1) = \dot{\tilde{\rho}}_1 \Big[f_1 - m\ddot{\rho}_1^d - m\rho_1 \Omega_1 \big(e_3^\times\big)^2 \Omega_1 \\ &+ m g e_3^{\mathrm{T}} \Gamma_1 + k\tilde{\rho}_1 \Big] + \tilde{\Omega}_1^{\mathrm{T}} \Big[\tau_1 - R_1^{\mathrm{T}} R_P \tau_{D_1} - \Omega_1^d \times J_1(\rho_1)\Omega_1 \\ &- J_1(\rho_1)\dot{\Omega}_1^d + m\rho_1\dot{\rho}_1\big(e_3^\times\big)^2\big(\Omega_1 + \Omega_1^d\big) + m g \rho_1 e_3^\times \Gamma_1 \\ &+ \Phi'\big(\mathrm{tr}(A - A Q_1)\big)(R_1^d)^{\mathrm{T}} S(Q_1) \Big], \end{aligned} \tag{27}$$

where $\Gamma_1 = R_1^{\mathrm{T}} e_3$ is the inertial z-axis direction in the stance leg's body-fixed frame and

$$S(Q) = \sum_{i=1}^{3} a_i Q^{\mathrm{T}} e_i \times e_i. \tag{28}$$

The time derivative of V_P along stance dynamics (7) is:

$$\frac{\mathrm{d}}{\mathrm{d}t}V_P(Q_P,\tilde{\Omega}_P,s,\tilde{s},\dot{\tilde{s}}) = \tilde{\Omega}_P^{\mathrm{T}}\Big[\tau_{D_1} - R_P^{\mathrm{T}}R_2\tau_{D_2} - J_P(s)\dot{\Omega}_P^d - \Omega_P^d \times J_P(s)\Omega_P - \frac{1}{2}N(s,\dot{s})\big(\Omega_P+\Omega_P^d\big) + \Phi'\big(\mathrm{tr}(A-AQ_P)\big)(R_P^d)^{\mathrm{T}}S(Q_P)\Big] + \dot{\tilde{s}}^{\mathrm{T}}\Big[u_s + L(s,\Omega_P) - 2m_P\ddot{s}^d + P\tilde{s}\Big]. \quad (29)$$

where $N(s,\dot{s}) = \frac{\mathrm{d}}{\mathrm{d}t}K_P(s)$ and $\dot{s}^{\mathrm{T}}L(s,\Omega_P) = \frac{1}{2}\Omega_P^{\mathrm{T}}N(s,\dot{s})\Omega_P$. Finally, the time derivative of V_{L_2} along dynamics (7) is

$$\frac{\mathrm{d}}{\mathrm{d}t}V_{L_2}(Q_2,\tilde{\Omega}_2) = \frac{1}{2}\tilde{\Omega}_2^{\mathrm{T}}\Big(-\Omega_2^d \times J_{L_0}\Omega_2 + \tau_{D_2} - J_{L_0}\dot{\Omega}_2^d + \Phi'\big(\mathrm{tr}(A-AQ_2)\big)(R_2^d)^{\mathrm{T}}S(Q_2)\Big). \quad (30)$$

The expressions (27), (29), and (30) lead to the control scheme given by the following statement.

Theorem 1. *Let $\ell > 0$ and let $D_1, D_P, D_2 \in \mathbb{R}^{3\times3}$ be positive definite matrices. Then the tracking control laws*

$$f_1 = m\ddot{\rho}_1^d + m\rho_1\Omega_1^T\big(e_3^\times\big)^2\Omega_1 - mge_3^T\Gamma_1 - k\tilde{\rho}_1 - \ell\dot{\tilde{\rho}}_1, \quad (31)$$

$$\tau_1 = R_1^TR_P\tau_{D_1} + J_1(\rho_1)\dot{\Omega}_1^d + \Omega_1^d \times J_1(\rho_1)\Omega_1 - mg\rho_1e_3^\times\Gamma_1 - m\rho_1\dot{\rho}_1\big(e_3^\times\big)^2\big(\Omega_1+\Omega_1^d\big) - \Phi'\big(tr(A-AQ_1)\big)(R_1^d)^TS(Q_1) - D_1\tilde{\Omega}_1, \quad (32)$$

$$\tau_{D_1} = R_P^TR_2\tau_{D_2} + \Omega_P^d \times J_P(s)\Omega_P + J_P(s)\dot{\Omega}_P^d - D_P\tilde{\Omega}_P + \frac{1}{2}N(s,\dot{s})\big(\Omega_P+\Omega_P^d\big) - \Phi'\big(tr(A-AQ_P)\big)(R_P^d)^TS(Q_P), \quad (33)$$

$$u_s = 2m_P\ddot{s}^d - L(s,\Omega_P) - P\tilde{s} - Q\dot{\tilde{s}}, \quad (34)$$

$$\tau_{D_2} = \Omega_2^d \times J_{L_0}\Omega_2 + J_{L_0}\dot{\Omega}_2^d - D_2\tilde{\Omega}_2 - \Phi'\big(tr(A-AQ_2)\big)(R_2^d)^TS(Q_2), \quad (35)$$

asymptotically stabilize the desired state trajectory given by equations (13)-(14)*. Further, the domain of convergence of this trajectory is almost global in the state space in the absence of control constraints and disturbance inputs.*

Proof. Consider the Lyapunov function

$$V(\tilde{\rho}_1,Q_1,\dot{\tilde{\rho}}_1,\tilde{\Omega}_1,Q_P,\Omega_P,s,\dot{s},Q_2,\tilde{\Omega}_2) = V_{L_1}(\rho_1,\tilde{\rho}_1,Q_1,\dot{\tilde{\rho}}_1,\tilde{\Omega}_1) + V_P(Q_P,\tilde{\Omega}_P,s,\tilde{s},\dot{\tilde{s}}) + V_{L_2}(Q_2,\tilde{\Omega}_2), \quad (36)$$

which captures the three coupled components (stance leg, torso, and swing leg), of the RMB. This time derivative is obtained by substituting expressions (27), (29) and (30) for $\dot{V}_{L_1}$, $\dot{V}_P$, and $\dot{V}_{L_2}$ respectively, along with substituting the control laws (31)-(35). This makes the time derivative of the Lyapunov function negative semi-definite:

$$\dot{V}(\dot{\tilde{\rho}}_1,\tilde{\Omega}_1,\tilde{\Omega}_P,\dot{\tilde{s}},\tilde{\Omega}_2) = -\ell\dot{\tilde{\rho}}_1^2 - \tilde{\Omega}_1^{\mathrm{T}}D_1\tilde{\Omega}_1 - \tilde{\Omega}_P^{\mathrm{T}}D_P\tilde{\Omega}_P - \dot{\tilde{s}}^{\mathrm{T}}Q\dot{\tilde{s}} - \tilde{\Omega}_2^{\mathrm{T}}D_2\tilde{\Omega}_2. \quad (37)$$

As the desired motion trajectories given by (13)-(14) are bounded and continuous, V as given by (36) is positive definite and is bounded above and below by suitably chosen positive definite functions of the trajectory tracking errors. Thereafter, invoking the invariance-like principle given by Theorem 8.4 in [19], one concludes that $\dot{V}$ converges asymptotically to zero. Thus, the positive limit set for the feedback tracking control system is a subset of

$$\dot{V}^{-1}(0) = \big\{(\tilde{\rho}_1,Q_1,\dot{\tilde{\rho}}_1,\tilde{\Omega}_1,Q_P,\Omega_P,\dot{\tilde{s}},Q_2,\tilde{\Omega}_2) : \dot{\tilde{\rho}}_1 = 0,\ \tilde{\Omega}_1 = 0,\ \tilde{\Omega}_P = 0,\ \dot{\tilde{s}} = 0,\ \tilde{\Omega}_2 = 0\big\}. \quad (38)$$

In the set $\dot{V}^{-1}(0)$, the feedback dynamics is restricted to

$$\tilde{\rho}_1 = 0,\ \Phi'\big(\mathrm{tr}(A-AQ_1)\big) = 0,\ \Phi'\big(\mathrm{tr}(A-AQ_P)\big) = 0,\ \tilde{s} = 0,\ \text{and } \Phi'\big(\mathrm{tr}(A-AQ_2)\big) = 0, \quad (39)$$

which characterizes the positive limit set of the feedback tracking system. Note that within the set of four critical points $\mathcal{E}_c$ of $\Phi\big(\mathrm{tr}(A-AQ)\big)$, it can be shown [20], [21] that $Q = I$ is the minimum, while the other points ($Q \in \mathcal{E}_c \setminus I$) are non-degenerate critical points. As $\dot{V} \leq 0$ for the feedback system, the only stable subset of the positive limit set is when the actual motion tracks the desired motion,

$$\tilde{\rho}_1 = 0,\ Q_1 = I,\ Q_P = I,\ \tilde{s} = 0,\ \text{and } Q_2 = I. \quad (40)$$

The other subsets (corresponding to $Q_1, Q_P, Q_2 \in \mathcal{E}_c \setminus I$) are unstable, although they may have stable subsets. Except for trajectories that start on these stable subsets of the positive limit set, all other state trajectories converge asymptotically to the desired state trajectory, which makes it asymptotically stable with an almost global domain of attraction. □

IV. Numerical Results

To illustrate the performance of the controller, we demonstrate (a) walking in a straight line, (b) walking towards a goal location, and (c) walking in a circle. In all cases, we choose a constant desired torso angle leaning forward, this is in contrast to (14) to simplify velocity and acceleration computation. The mass and inertia properties of the reaction mass biped are chosen to be similar to that of a NAO robot:

$$m_L = 0.882\text{kg}, J_{L_0} = 0.5\text{diag}\{0.98, 0.91, 0.63\}\text{kg-m}^2,$$
$$m_P = 0.32\text{kg}, J_{P_0} = \begin{bmatrix} 0.2126 & 0.0004 & -0.0002 \\ 0.0004 & 0.2042 & 0.0010 \\ -0.0002 & 0.0010 & 0.2246 \end{bmatrix}\text{kg-m}^2.$$

Walking in a straight line: We chose $\zeta_1 = e_2, R_{10} = R_{20} = I$, and $T = 1$s as in (13). Moreover, we introduce a constant phase offset in the angles for R_1^d, R_2^d to enable the swing legs to swing from -15° to 15°. Figure 2a illustrates a snapshot and the tracking errors.

Walking towards a goal: We modify the walking in a straight line controller given above, with an event-based modification of R_{10}, R_{20} at each impact to change the heading of the biped. Figure 2b illustrates a snapshot and the tracking errors. Note that at each impact, the desired yaw instantaneously changes and the controller is able to regulate the errors asymptotically within a step.

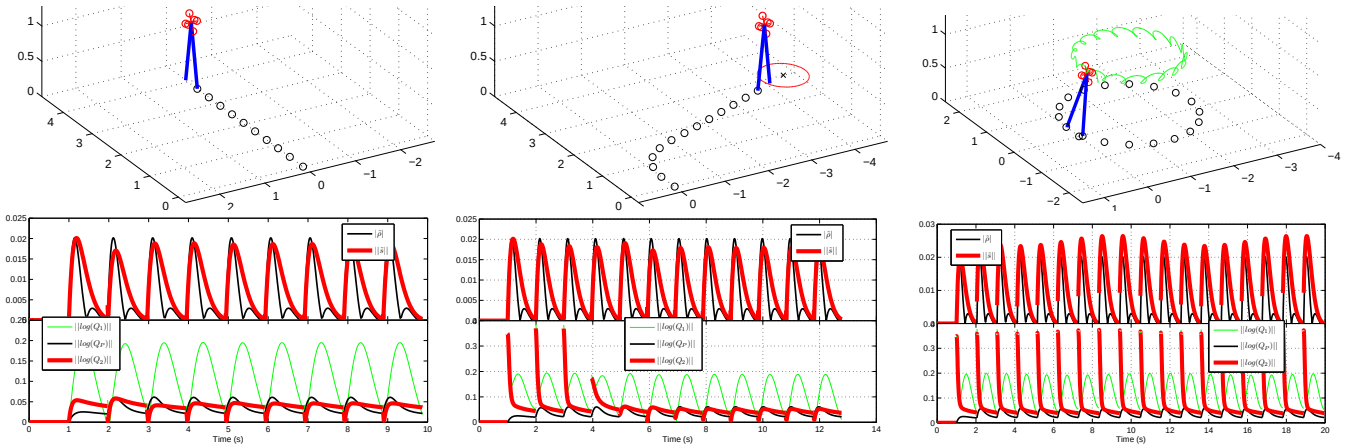

(a) Walking Straight (b) Walking to a Goal (c) Walking in a Circle

Fig. 2: Numerical simulations of the controller for (a) Walking along a straight line, (b) Walking towards a goal location by changing the yaw-angle in an event-based step-to-step manner, and (c) Walking in a circle while leaning inwards, with the hip position shown in green. In all the cases, the controller tracking errors are illustrated. These include the errors defined in (23), namely $|\tilde{\rho}_1|$, $||\tilde{s}||$, $||\log(Q_1)||$, $||\log(Q_P)||$, and $||\log(Q_2)||$. As can be seen, the controller reduces the error during the continuous stance-phase, while the impacts causes the errors to increase. The simulation begins with zero initial errors, and hence the errors during the first step remain zero.

Walking in a circle: We employ the walking towards a goal controller as above, but modify R_{10}, R_{20} by a fixed amount at each impact in order to lean the body into the turn. Figure 2c illustrates a snapshot (with the hip position demonstrating the body lean) and the tracking errors. Note that instead of modifying R_{10}, R_{20}, we could have modified ζ_1, ζ_2 too.

V. Conclusion

A variable inertia multibody biped model that can model highly dynamic bipedal locomotion was presented. An asymptotically stable trajectory tracking control scheme with an almost global domain of convergence is used to control this biped for walking in curvilinear trajectories.

References

[1] S.-H. Lee and A. Goswami, "Reaction mass pendulum (RMP): An explicit model for centroidal angular momentum of humanoid robots," in *IEEE International Conference on Robotics and Automation*, April 2007, Rome, Italy, pp. 4667–4672.

[2] A. Dutta and A. Goswami, "Human postural model that captures rotational inertia,," in *American Society of Biomechanics*, August 2010, Providence, Rhode Island, USA.

[3] A. K. Sanyal and A. Goswami, "Dynamics and balance control of the reaction mass pendulum (rmp): A 3d multibody pendulum with variable body inertia," *ASME Journal of Dynamic Systems, Measurement and Control*, vol. 136, no. 2, p. paper 021002, 2014.

[4] S. Kajita and K. Tani, "Study of dynamic biped locomotion on rugged terrain," in *IEEE International Conference on Robotics and Automation*, 1991, pp. 1405–1411.

[5] S. Kajita, F. Kanehiro, K. Kaneko, K. Yokoi, and H. Hirukawa, "The 3D linear inverted pendulum model: A simple modeling for a biped walking pattern generator," in *IEEE/RSJ International Conference on Intelligent Robots and Systems*, 2001, Maui, Hawaii, pp. 239–246.

[6] S. Kajita, F. Kanehiro, K. Kaneko, K. Fujiwara, K. Harada, K. Yokoi, and H. Hirukawa, "Biped walking pattern generation by using preview control of zero-moment point," in *IEEE International Conference on Robotics and Automation*, 2003, Taipei, Taiwan, pp. 1620–1626.

[7] T. Sugihara and Y. Nakamura, "Variable impedant inverted pendulum model control for a seamless contact phase transition on humanoid robot," in *IEEE International Conference on Humanoid Robots*, Oct 2003, Germany, pp. 0–0.

[8] R. Altendorfer, U. Saranli, H. Komsuoglu, D. Koditschek, H. B. Brown, M. Buehler, N. Moore, D. McMordie, and R. Full, "Evidence for spring loaded inverted pendulum running in a hexapod robot," in *Experimental Robotics VII*, D. Rus and S. Singh, Eds. Springer-Verlag, 2001, pp. 291 – 302.

[9] T. Komura, H. Leung, S. Kudoh, and J. Kuffner, "A feedback controller for biped humanoids that can counteract large perturbations during gait," in *IEEE International Conference on Robotics and Automation*, 2005, Barcelona, Spain, pp. 2001–2007.

[10] T. Komura, A. Nagano, H. Leung, and Y. Shinagawa, "Simulating pathological gait using the enhanced linear inverted pendulum model," *IEEE Transactions on Biomedical Engineering*, vol. 52, no. 9, pp. 1502–1513, 2005, September.

[11] R. D. Gregg and M. W. Spong, "Reduction-based control of three-dimensional bipedal walking robots," *The International Journal of Robotics Research*, vol. 29, no. 6, pp. 680–702, May 2010.

[12] R. Gregg, A. Tilton, S. Candido, T. Bretl, and M. Spong, "Control and planning of 3d dynamic walking with asymptotically stable gait primitives," *IEEE Transactions on Robotics*, vol. 28, no. 6, pp. 1415–1423, 2012.

[13] R. Sinnet and A. D. Ames, "3d bipedal walking with knees and feet: A hybrid geometric approach," in *IEEE Conference on Decision and Control*, December 2009, pp. 3208–3213.

[14] K. A. Hamed, B. G. Buss, and J. W. Grizzle, "Continous-time controllers for stabilizing periodic orbits of hybrid systems: application to an underactuated 3d bipedal robot," in *IEEE Conference on Decision and Control*, December to appear, 2014.

[15] J. W. Grizzle, C. Chevallereau, A. Ames, and R. Sinnet, "3d bipedal robotic walking: Models, feedback control, and open problems," in *IFAC Symposium on Nonlinear Control Systems*, Bologna, Italy, September 2010.

[16] C.-L. Shih, J. W. Grizzle, and C. Chevallereau, "From stable walking to steering of a 3d bipedal robot with passive point feet," *Robotica*, vol. 30, no. 7, pp. 1119–1130, 2012.

[17] R. Abraham and J. E. Marsden, *Foundations of Mechanics*, 2nd ed. New York, NY: Benjamin/Cummings Publishing Company, 1978.

[18] Y. Hürmüzlü and T. Chang, "Rigid body collisions of a special class of planar kinematic chains," *IEEE Transactions on Systems, Man and Cybernetics*, vol. 22, no. 5, pp. 964–71, 1992.

[19] H. K. Khalil, *Nonlinear Systems*, 3rd ed. Englewood Cliffs, NJ: Prentice Hall, 2002.

[20] A. K. Sanyal, A. Fosbury, N. A. Chaturvedi, and D. S. Bernstein, "Inertia-free spacecraft attitude trajectory tracking with disturbance rejection and almost global stabilization," *AIAA Journal of Guidance, Control and Dynamics*, vol. 32, no. 2, pp. 1167–1178, Feb 2009.

[21] N. A. Chaturvedi, A. K. Sanyal, and N. H. McClamroch, "Rigid-Body Attitude Control: Using rotation matrices for continuous, singularity-free control laws," *IEEE Control Systems Magazine*, vol. 31, no. 3, pp. 30–51, June 2011.